DISSIMILAR METAL WELDING USING Nd:YAG PULSED LASER

N. D. PANDEY, N. ARORA*, ARVIND BHARTI and P. CHAKRAVORTY*

Defence Metallurgical Research Laboratory, Hyderabad 500 058, India
*Department of Mechanical and Industrial Engineering
Indian Institute of Technology, Roorkee 247 667, India

ABSTRACT

Pulsed laser beam welding is a non-traditional technique for welding of a wide range of dissimilar metals. For optimizing parameters for welding of Permendur 49 with stainless steel-304, a detailed parametric study has been conducted using an industrial pulsed Nd :YAG laser. Effect of welding parameters on welds has been studied for controlling weld properties. Based on microscopic examination of simulated (bead-on-plate) welds on the constituents, an expert system has been developed. The expert system has been experimentally validated.

Key Words: Pulsed laser beam welding, Dissimilar metal welding, Pulsed Nd :YAG laser, Permendur-49, Stainless steel-304, Expert system, Microstructure, Tensile strength

INTRODUCTION

Dissimilar metal welding (DMW) has potential to let a design engineer use different materials at different locations of a component in order to improve its functional efficiency. It has received significant attention in the last few years [1-7]. However, the welding of dissimilar metals often presents a difficult-to-overcome technological problem in terms of weld integrity. The resultant weld may contain various flaws like porosity, cracking, underfill etc. or it may become brittle immediately after welding or after postweld heat treatment [3]: Therefore, in order to obtain a sound DMW, the following physical, metallurgical, corrosion and mechanical properties of the constituents must be examined. The physical properties to be considered are coefficient of thermal expansion, heat diffusivity and melting range. The metallurgical aspects include solubility limits, secondary phases and phase stability. The corrosion factors are galvanic, pitting and crevice types of corrosions, corrosion fatigue, stress corrosion cracking and surface area ratio. The mechanical properties involve tensile, stress rupture and creep, fatigue, impact, hardness properties [2, 4].

A sound DMW can be produced by the following three approaches in spite of the dissimilarity of properties of constituent metals. The first is to create a transition zone between the surfaces to be joined whose properties are such that they fall between the properties of the constituent metals. Use of interlayer of an appropriate intermediate metal(s) between the faying surfaces helps creating such zone. Next is to modify vulnerable zone by pre and post weld heat treatments. Limiting the vulnerable zone by applying the suitable welding technique and weld design is the last approach [1-2].

Table 1 : Comparison of the Characteristics of LBW and other suitable processes for DMW

Characteristics	Welding Process			
	LBW	EBW	GTAW	RW
Heat Input	Low	Moderate	Moderate	Very High
Weld Quality	Excellent	Excellent	Good	Excelllent
Welding Speed	High	High	Moderate	Moderate
Operating Cost	Moderate	Moderate	Moderate	Low
Tooling Cost	Low	High	High	Moderate
Controllability	Very Good	Good	Low	Fair
Ease of Automation	Excellent	Good		Fair
Range of Dissimilar Materials to be welded	Wide	Wide	Narrow	Narrow

Many welding techniques like gas metal arc welding (GMAW), gas tungsten arc welding (GTAW), shielded metal arc welding (SMAW), resistance welding (RW), diffusion bonding (DB), plasma arc welding (PAW), electron beam welding (EBW) and laser beam welding (LBW) are utilized for DMW [3-6]. Characteristics of LBW are compared with other welding processes in Table 1 [7-8]. LBW has only one true competitor, i.e. EBW. However, the LBW is superior to EBW in the sense that it is unaffected by magnetic material, no vacuum is needed during welding, tooling cost is low and automation is easy [9].

Pulsed LBW utilizes the third approach (discussed above) in producing good. DMWs in the wide range of metals as shown in Table 2[8] due to its characteristics like well defined focal spot and high power density. Well-defined focal spot allows control of dilution of the weld pool by the constituents. High power density (10^{10}-10^{12} $W.m^{-2}$) of the laser beam allows high speed welding. Hence, the size of weld and heat affected zone (HAZ) are smaller. The offshoots of high welding speed are rapid solidification of the weld pool and formation of compressive residual stresses at the weld surface. The former may suppress formation of deleterious phases in the weld and the latter can improve its fatigue properties.

Many applications of strategical importance demand that Permendur 49 (P-49, a soft magnetic and strategically important metal) and stainless steel 304 (SS-304) are welded in vicinity of a thermal sensitive device. Due to low heat input and insensitivity to magnetic field, the pulsed LBW is the most suitable welding technique for this [10]. We are presenting here, the important findings of our study of the LBW of P-49 and SS-304 using a pulsed Nd :YAG laser. Details of an expert system developed on the basis of the experimental data and its experimental validation are also included in this paper.

EXPERIMENTAL STUDIES

A 400 W pulsed Nd:YAG laser coupled with a 5-axis CNC work station is used' for the experiments. The raw laser beam has been focussed using a 101.6mm focal length quartz lens. The radiation of Nd :YAG laser falls in the infrared region of the spectrum, hence is invisible. This creates problem in

Table 2 : Performance of LBW for DMW of different dissimilar metal combinations [8]

	W	Ta	Mo	Cr	Co	Ti	Be	Fe	Pt	Ni	Pd	Cu	Au	Ag	Mg	Al	Zn	Cd	Pb	Sn
W																				
Ta	E																			
Mo	E	E									E	Excellent								
Cr	E	P	E								G	Good								
Co	F	P	F	G							F	Fair								
Ti	F	E	E	G	F						P	Poor								
Be	P	P	P	P	F	P														
Fe	F	F	G	E	E	F	F													
Pt	G	F	G	G	E	F	P	G												
Nl	F	G	F	G	E	P	F	G	E											
Pd	F	G	G	G	E	F	F	G	E	E										
Cu	P	P	P	P	F	F	F	F	E	E	E									
Au	-	-	P	F	P	F	F	F	E	E	E	E								
Ag	P	P	P	P	P	F	P	P	F	P	E	F	E							
Mg	P	-	P	E	P	P	P	P	P	P	P	F	F	F						
Al	P	P	P	P	F	F	P	F	P	F	P	F	F	F	F					
Zn	P	-	P	P	F	P	P	F	P	F	F	G	F	G	P	F				
Cd	-	-	-	P	P	P	-	P	F	F	F	P	F	G	E	P	P			
Pb	P	-	P	P	P	P	-	P	P	P	P	P	P	P	P	P	P	P		
Sn	P	P	P	P	P	P	P	P	F	P	F	P	F	F	P	P	P	P	F	

Table 3 : Characteristics of Laser Welds of Stainless Steel-304

Pulse width (ms)	Average Power (W)	Speed (mm.min^{-1})	Apparent beam diameter (μm)		
			16	600	1200
1	50	60	G		D
	110		D		DE
2	50	60	DE		G
	125		D		DE
3	50	60	D		G
		195	D		G
	100	60	DE		G
		195	DE		G
	125	60	DE		G
		195	DE		G,G
4	50	60	G	G	G
		120		G	G
		195	G	G	G
		240	G	G	G
	75	60	D	D	G
		120		G	G
		195	G	G	G
		240	G	G	G
	100	60	D	D	G
		120		G	G
		195	DE	G	G
		240	DE	G	G
	125	60	D,G	D	G,G
		120		D	G
		195	DE,G	G	G,G
		240	DE	G	G
	150	60	D		D
		195	G		G
5	50	60	G		D
		195	G		G
		240	G		G
	100	60	D		D
		195	G		G
		240	G		G
	125	60	D		G
		195	G		G
		240	G		G
6	50	60	G		G
	125	60	G		G
7	50	60	G		G
	110	60	G		G

G : Good, D : Defective, DE : Excessively Defective

measuring beam diameter. Therefore, values of the beam diameters (at focus and away from it) have been calculated theoretically [11].

SS-304 is an 18Cr-8Ni (wt.%) stainless steel and the nominal composition of P-49 is Fe-49Co-2V (wt.%).

The surface of the SS-304 and P-49 sheets has been polished with No. 400 emery paper to induce surface roughness for better absorp-

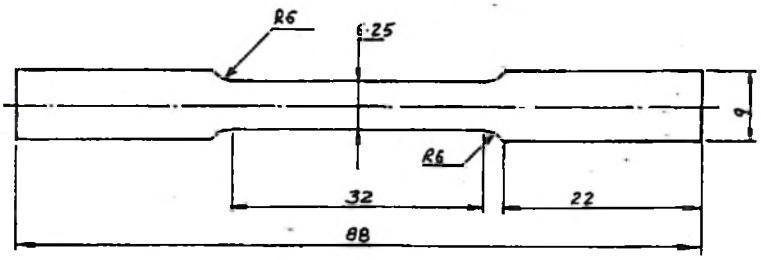

Fig.1 : Tensile test specimen (all dimensions in mm).

tion of laser. The average surface roughness of the polished specimens has been measured on Mitutoyo Surftest-211 and found to be 0.5 μm. Argon gas is delivered coaxially at 20 kPa (at cylinder head) for shielding the weld pool. Parametric ranges of the variables used in the welding study are as follows: average power from 50 to 150 W, welding speed from 60 to 240 mm.min^{-1}, pulse width from 1 to 7 ms and beam diameter from 16μm to 1.2 mm. Simulated (bead-on plate) welds on constituent metals and dissimilar metal welds have been produced using the above parameters.

The transverse sections of welds have been prepared using standard metallographic methods. The metallographic specimens have been etched using a reagent having 200ml Methanol + 100ml HCl + 100ml Distilled H_20 + 5ml HNO_3 + 7g $FeCl_3$ + 2g $CuCl_2$ and examined under a metallurgical microscope. Tensile test specimens as per the drawing shown in Fig. 1 have been machined by wire cut - electro discharge machining (EDM). Tensile testing of the specimens has been carried out on a universal testing machine (UTM).

A Microsoft Windows based Visual Basic 6.0 software has been used for development of the expert system.

RESULTS AND DISCUSSION

Characteristics of the weld beads on SS-304 and P-49 over the entire parametric range is given in Tables 3 and 4. They are based on the microscopic examination of about 105 welds on SS-304 and about 64 welds on P-49. The welds have been classified into three categories (a) good (G), (b) defective (D) and (c) excessively defective (DE). The good welds have no underfill and insignificant porosity. The welds under the category of defective welds have underfill in the range of 40 to 250 μm and/or few pores having diameter in the range from 40 to 80 μm. Excessively defective welds are those containing underfill and porosity more than the specified values under the category of the defective welds. The underfill is measured where it is maximum on the transverse section of the welds. Examples of the typical good, defective and excessively defective welds in SS-304 and P-49 are shown in Figures 2 and 3 respectively.

Study of Tables 3-4 shows that majority of the good welds can be obtained when laser pulse width is above 3 ms and welding is carried out using defocussed beam. This is because the combinations of lower pulse widths ($\leq$ 3ms) and lower beam diameter (16 μm) generate high power density (in the order of tens of TW.m^{-2}), which causes excessive vaporization and leads to other defects in the welds. In general, the good welds can be obtained with laser power density of the order of 10^{-1} TW.m^{-2}. This is in agreement with the literature also [12]. The good welds have smooth surface finish and negligible HAZ. Mazumder [13] has compared properties of the welds produced by LBW, EBW, GTAW and PAW and reported that the LBW produces welds with minimum distortion and HAZ, and smoother surface at higher welding speed.

Variation in Weld Geometry

Depth (d) and width (w) of the welds of SS-304 and P-49 have been plotted as functions of average power, welding speed, pulse width and beam diameter in Figures 4-9. Different LBW parameters affect weld geometry differently. By manipulating the parameters, it is possible to control depth of good welds from

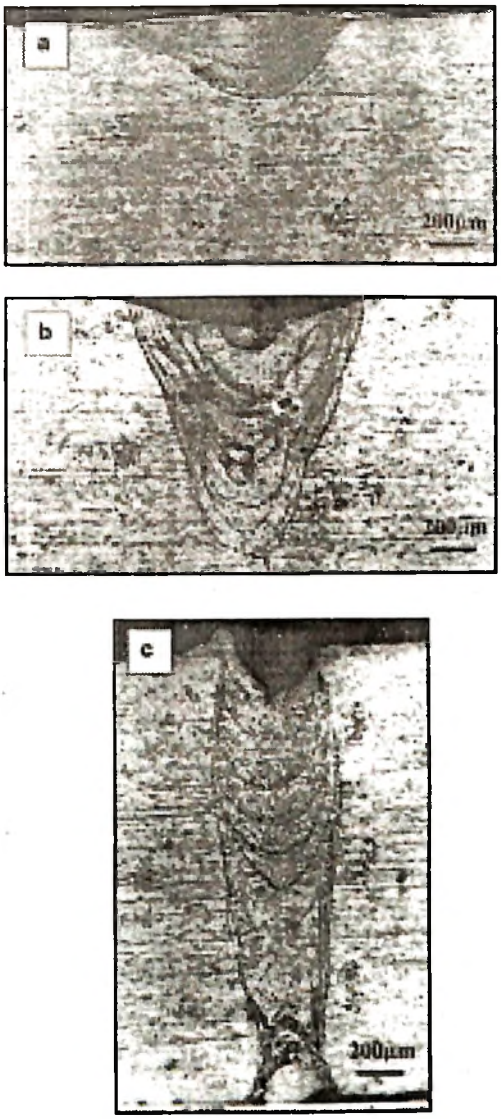

Fig.2 : Microstructure of different representative welds in SS-304 (a) good (b) defective and (c) excessively defective.

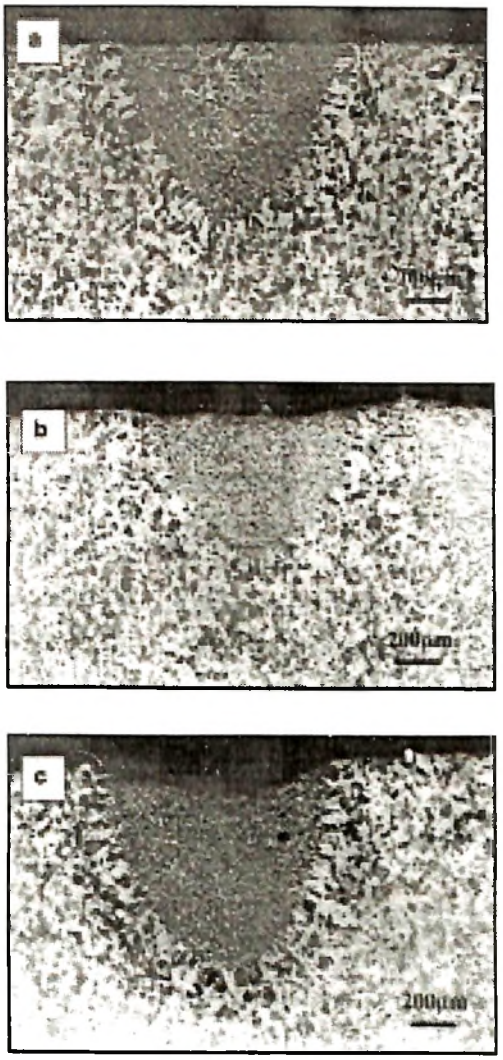

Fig.3 : Microstructure of different representative welds in P-49 (a) good (b) defective and (c) excessively defective.

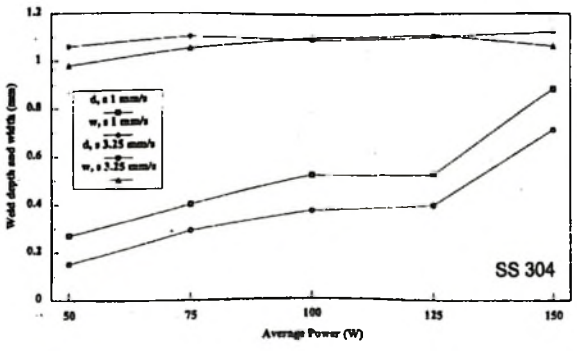

Fig.4 : Depth and width of SS-304 welds as a function of the average power for 4ms pulse width and 1.2mm beam diameter.

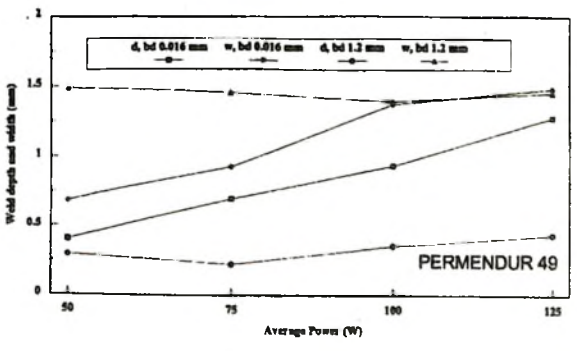

Fig.5 : Depth and width of Permendur 49 welds as a function of the average power for 4ms pulse width and 60mm. min^{-1} speed.

0.25 to 1.25 mm and width of good welds from 0.5 to 1.5 mm for SS-304 and P-49. In general the d increases with the average laser power (Figures 4-5). The w increases with the average laser power for small beam diameter (16 μm). However, the w either marginally decreases or remains constant for larger beam diameter (1.2 mm). The rate of increase of d is nearly double after 125 W for SS-304 welds. This is because laser energy absorption by the materials increases with the laser power [14], leading to increase in d and w. However, above certain power density, mode of welding changes from conduction limited to keyhole [15]. It may be a reason for sudden change in the rate of increase of d beyond 125 W.

Effect of welding speed on d and w is shown in Figures 6-7. The d and w decrease with the increase in welding speed for P-49. The d and w are at their lowest value at 3.25 mm.s^{-1} speed for SS-304. With the increase in welding speed, laser-material interaction time decreases which results in decreasing available laser energy per unit volume of material. Hence, there is a decrease in d and w values with the decrease in welding speed.

The laser-material interaction also results in formation of plasma containing thermally induced charged particles and material vapor. The laser induced plasma (LIP) being opaque prevnts the laser beam to reach the base material and thereby affects the available laser energy [16]. We have observed that at 4 mm.s^{-1} speed, the LIP has been relatively attenuated which might have resulted in the increase of d at that speed.

Variations of d and w as functions of focussed beam diameters are shown in Figures 5 and 8. For higher power (125 W), d decreases and w increases with the increase in the beam diameter. The trend is less pronounced at lower power (5O W).

Effect of the increase in pulse width on d and w is fairly complicated as shown in Figure 9. It can be observed that there are two cycles of increase and decrease. As pulse width is increased from 1 to 2 ms, the d peaks. Further increase in pulse width up to 4 ms leads to fall in d. The d again peaks at 5ms and falls further with the increase in pulse width up to 7 ms. The trend is same for w, however, the variation is much less pronounced for lower powers (50 W). The overall trend is that an increase in pulse width leads to a decrease in d. In order to understand this behavior, we have to look at the physical picture of the prevailing heat transfer during welding. Distribution of energy per pulse for the shortest pulse (1 ms) and the longest (7 ms) pulse is shown schematically in Figure 10. Peak power, duty cycle, off time of duty cycle, peak surface temperature and thermal diffusion distance have been calculated [17-19] and given in Table-5. For shorter pulse more inter-pulse time is available for thermal

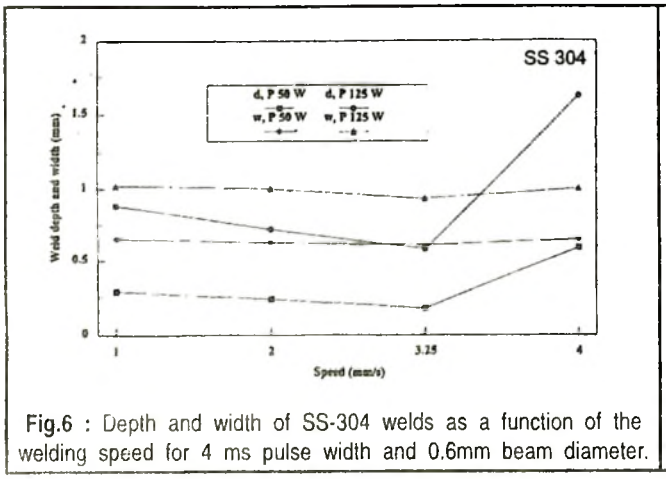

Fig.6 : Depth and width of SS-304 welds as a function of the welding speed for 4 ms pulse width and 0.6mm beam diameter.

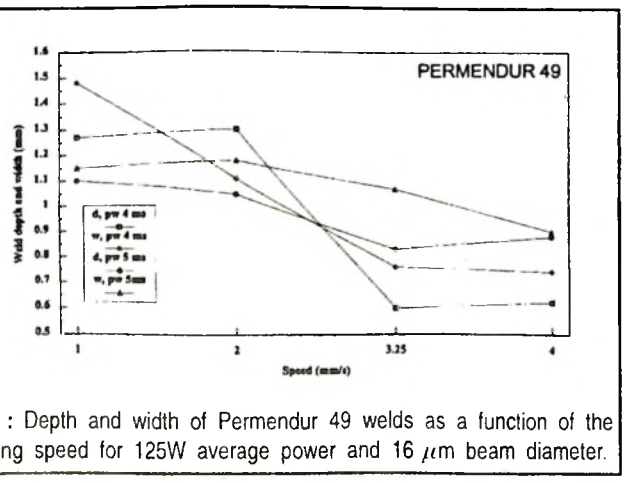

Fig.7 : Depth and width of Permendur 49 welds as a function of the welding speed for 125W average power and 16 μm beam diameter.

Table 4 : Characteristics of Laser Welds of Permendur 49

Pulse width (ms)	Average power (w)	Beam diameter (μm)	Speed (mm.min^{-1})			
			60	120	195	240
4	50	16	D	G	G	G
		1200	G	G	G	G
	75	16	D	D	D	G
		1200	G	G	G	G
	100	16	D	D	D	G
		1200	G	G	G	G
	125	16	D	D	DE	G
		1200	G	G	G	G
5	50	16	G	G	G	G
		1200	G	G	G	G
	75	16	D	D	G	G
		1200	G	G	G	G
	100	16	DE	G	G	G
		1200	G	G	G	G
	125	16	DE	DE	G	G
		1200	G	G	G	G

G : Good, D : Defective, DE : Excessively Defective

Table 5 : Peak power, duty cycle, off time of duty cycle, peak surface temperature and diffusion distance in SS-304 for different pulse widths

Pulse Width (ms)	Peak Power (kw)		Duty Cycle (%)	Duty Cycle Off-time (ms)	Peak surface Temp. for 125 w (X 10^6 ^{0}c)	Thermal Diffusion Distance (x10^{-4}m)
	For 50 W	For 125 W				
1	1.67	4.17	3	32.33	5.54	3.64
2	0.83	2.08	6	31.33	2.77	3.58
3	0.56	1.39	9	30.33	1.85	3.53
4	0.42	1.04	12	29.33	1.37	3.47
5	0.33	0.83	15	28.33	1.10	3.41
6	0.28	0.69	18	27.33	0.92	3.35
7	0.24	0.60	21	26.33	0.80	3.29

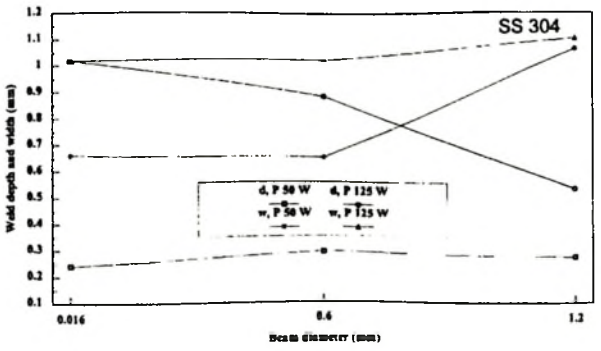

Fig.8 : Depth and width of SS-304 welds as a function of the beam diameter for 4 ms pulse width and 60mm.min^{-1} welding speed.

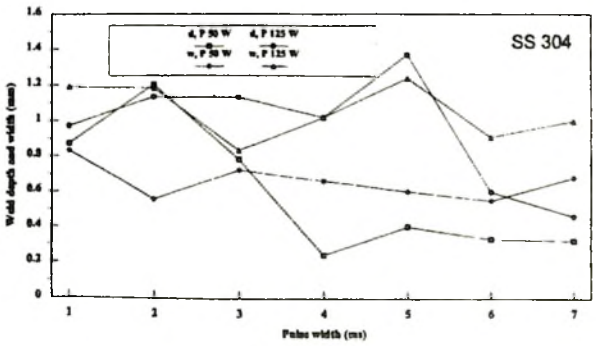

Fig.9 : Depth and width of SS-304 welds as a function of the pulse width for 16μm beam diameter and 60mm.min^{-1} weiding speed.

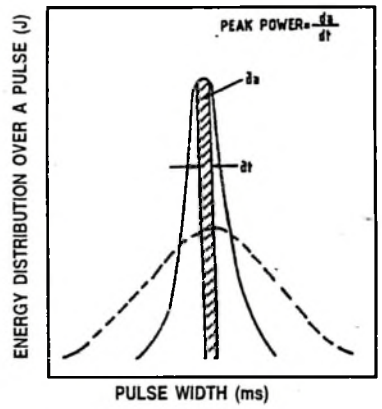

Fig.10 : Energy distribution over a pulse for two pulses of different pulse widths (shown schematically).

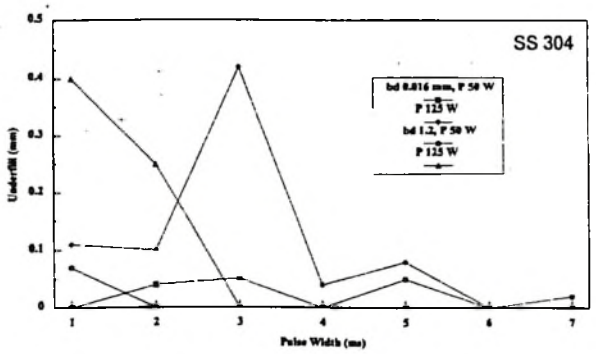

Fig.11 : Underfill of SS-304 welds as a function of the pulse width for 60mm.min^{-1} welding speed

diffusion. Hence, the relevant isotherm travels farther before next pulse delivers energy. Overall where peak power and peak temperature are higher, the resultant weld should show a larger d and w. This in general is true, e.g., d and w at 1 ms pulse for 125 W is 0.97 mm and 1.19 mm compared to 0.46 mm and 1.00 mm respectively at 7 ms pulse for the same power. However, in order to explain the peaks of d on intermediate values of pulse widths (Fig. 9), interaction of the residual heat of the previous pulse with the same of the incoming pulse has to be accounted for. We are computing them and those results will be published later.

The underfill has also been plotted as a function of pulse width (Fig. 11). It can be seen that the degree of underfill of welds decreases with the increase in pulse width. Welds produced at pulse widths ≥4 ms are less prone to defects caused by underfill.

Microstructure of Welds

Microstructures of the typical good, defective and excessively defective welds in SS-304 and P-49 are shown in Figures 2-3. It can be seen from Figure 2a, b and c that grain refinement takes place in weld zone of P-49. Heat affected zone (HAZ) is also present. HAZ is absent in SS-304 welds (Figures 3 a, b and c). Concentric curves are also seen in weld zone. One of the reasons of their formation is convection in the weld pool. Formation of the curves also depends on kinetic conditions of solidification prevailing in the weld pool and thermal properties of the material.

Design and Development of Expert System

A rule based expert system has been designed to facilitate quick retrieval of data [20]. The design of an expert system is based on the above mentioned various characteristics of the simulated welds. The VB++ v.6.0 is used as an Expert System Building Tool. The main logic of the expert system is different for similar and dissimilar combinations of thickness and constituent metals. The desired weld depth should be at least equal to the thickness of plate while welding plates of same thickness for producing satisfactory welds. While welding sheets of different thickness, the desired weld depth should be at least equal to the thickness of thinner plate. The flow chart of the expert system is shown in Figure 12. Flow chart shows that expert system starts from START command and logo (Fig. 13) of the expert system appears for 5 seconds, then it displays an input screen (Fig. 14). Through the input screen, user can select two dissimilar metals. Further the user has to select method of edge preparation. After that if user presses OK button, the expert system predicts the values of the LBW parameters in the form of an output screen as shown in Figure 15.

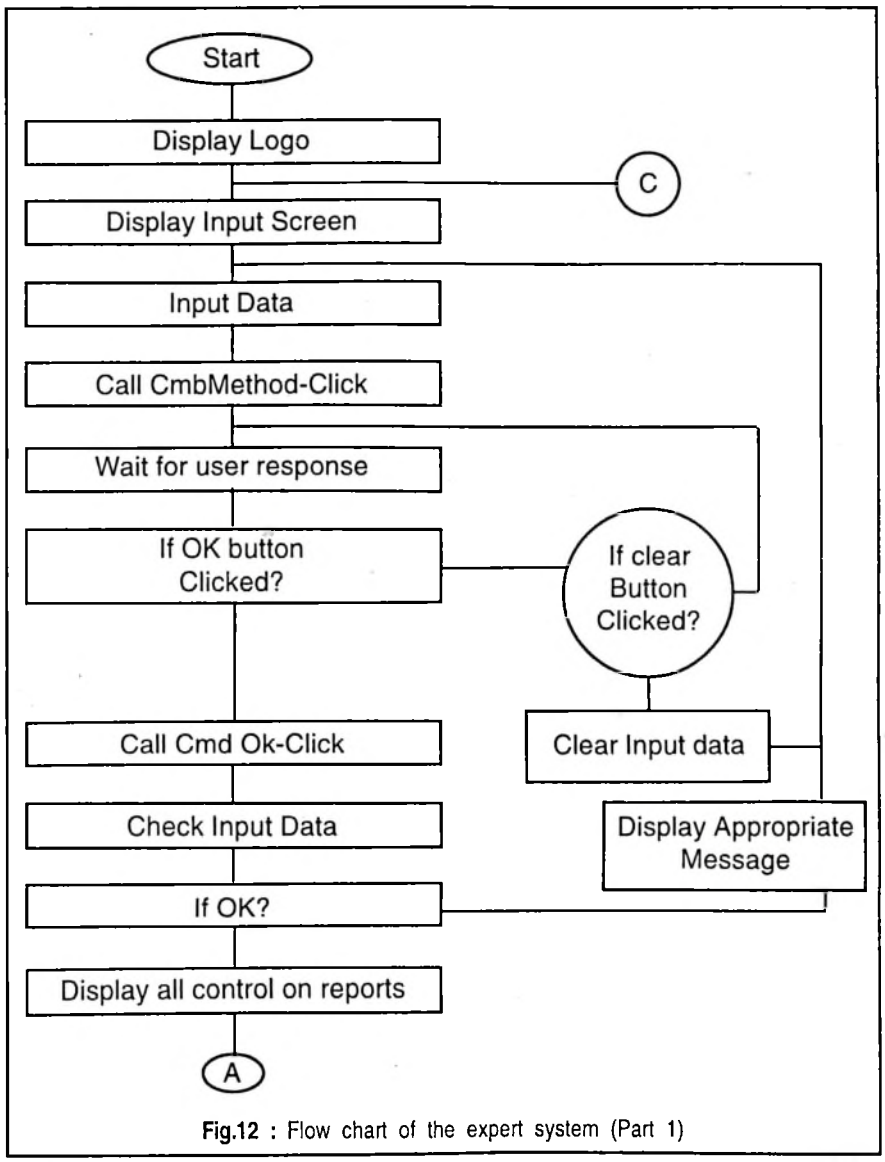

Fig.12 : Flow chart of the expert system (Part 1)

Experimental Validation of the Expert System

Validation of the expert system has been carried out in the following steps. In the input screen, we have selected the first material as Stainless Steel 304 and the second material as Permendur 49 (Fig. 14). The thickness (in mm) of first material has been chosen as 0.5 and of the second material as 2.6. The method of edge preparation has been selected as Grinding. After pressing the OK button, the output screen appears as Figure 15 giving various combinations of LBW parameters which shall result in a good DMW.

We have selected LBW parameters (pulse width 4 ms, average power 125 W, welding speed 60 mm.min^{-1} and beam diameter 1.2 mm) for butt welding of 0.5 mm thin SS 304 with 2.6 mm thick Permendur 49. The microstructure of the weld is shown in Figure 16a. It can be seen that resultant weld is sound and contains no porosity and cracking. Further, the microstructure is considerably different than that of the welds of constituent alloys. The weld pool is free from concentric curves. This is due to mixing of the alloys in the weld pool. No HAZ seems to be present on P-49 side. Grain refinement takes place in the weld. The weld has been tested for room temperature tensile strength. It has shown very good properties as it fractured in base metal (SS-304 side as seen in Fig. 16b). Based on the breaking load: 2 kN and assumed cross sectional area (calculated by' multiplying the thickness of the thinner sheet with the width of the tensile specimen in the middle of the gauge length) of the weld: 3 mm^2, the weld has shown 700 MPa ultimate tensile strength.

The expert system is effective for butt welding of thin (<1.5 mm) to thick sheets in combinations of P-49 and SS-304. However, the expert system is expandable for other dissimilar metal combinations and weld joint configurations also.

CONCLUSIONS

1. A strategically important dissimilar metal couple: Permendur-49/Stainless Steel-304 can be welded using a Nd :YAG pulsed laser.

2. Optimized combination of laser pulse widths between 3 ms to 7

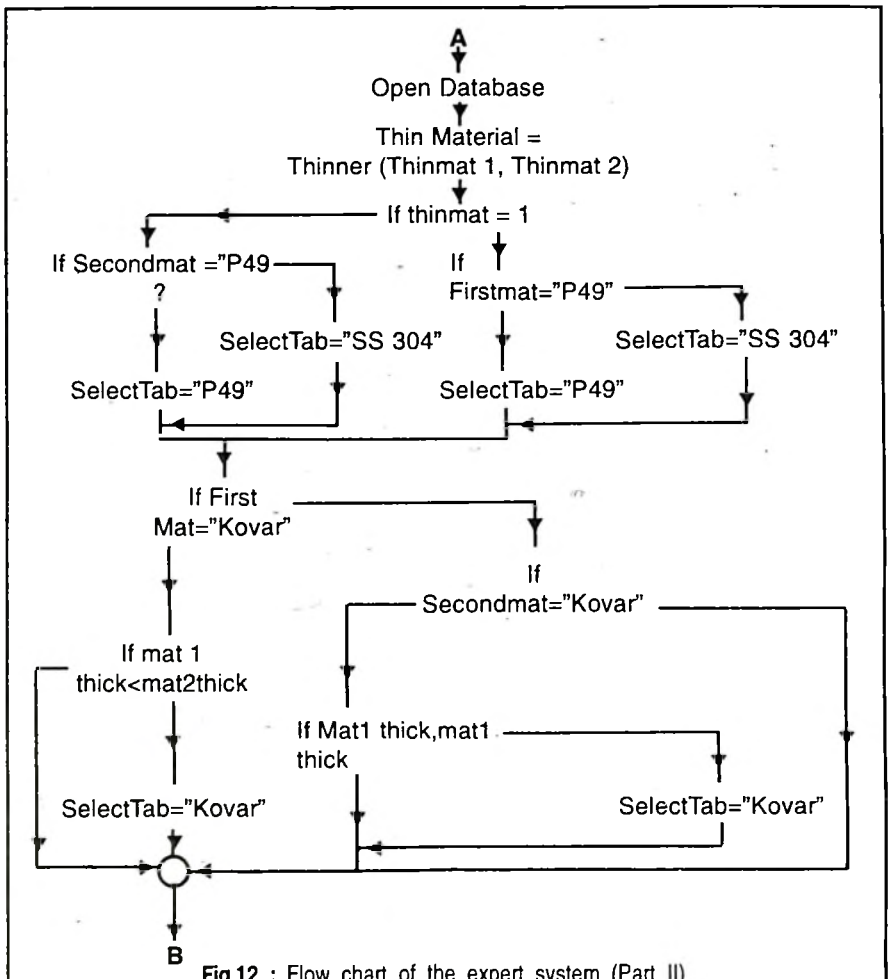

Fig.12 : Flow chart of the expert system (Part II)

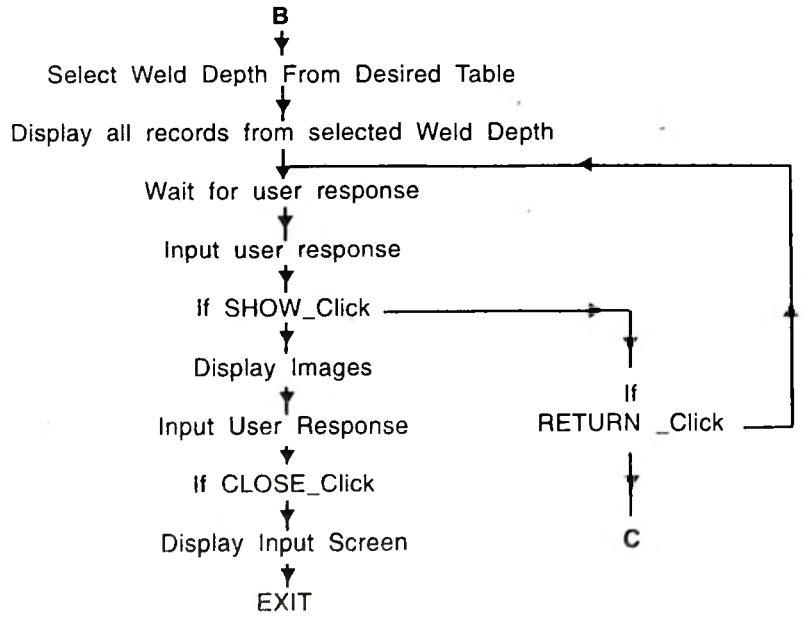

Fig.12 : Flow chart of the expert system (Part III and the last part)

ms and a defocussed laser beam can produce good welds.

3. An expert system developed during the present study, effectively predicts laser welding parameters for butt welding of similar and dissimilar thickness sheets of Permendur-49 and Stainless Steel-304.

ACKNOWLEDGEMENTS

The authors are grateful to Dr. D. Banerjee, Director, DMRL for constant encouragement and support. We are thankful to Dr. A.M. Sriramamurthy, Division Head and Shri K Mallikharjuna Rao, Group Head for general support. The work is carried out under general DRDO grants and is published with the permission of the Director, DMRL.

REFERENCES

1. D. Johnson, W. Penn and S. Bushik, Indus. Laser Review, April 1998, pp. 20-23.
2. A.K. Ghose and A. Joarder, Tools and Alloy Steels, 25(8), 1991, pp. 289-294.
3. R.E. Avery, Chem. Eng. Prog., 991, pp. 70-75
4. B. Irving, Weld. J., 1992, pp.27-33.
5. M.J. Nicholas and R.J. Lee, Metals and Materials, 1989, pp. 348-351.
6. G. Metzger and R. Lison, Weld. J., 1976, pp. 230s-240s.

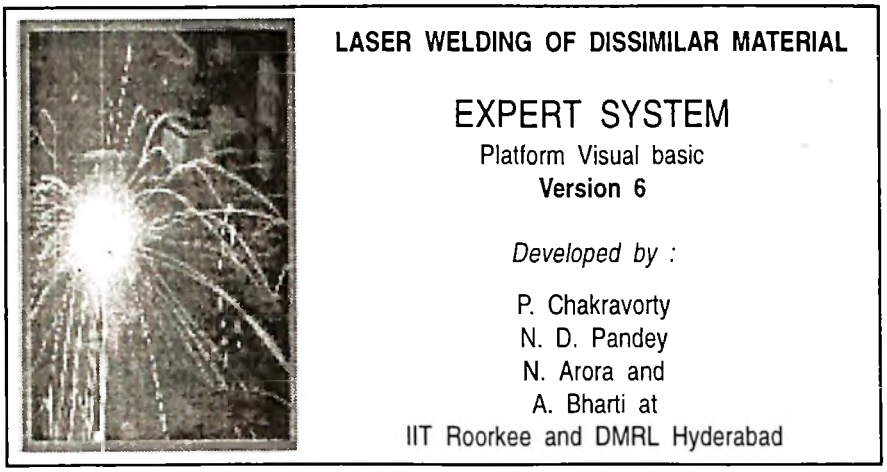

Fig.13 : Opening screen of the expert system

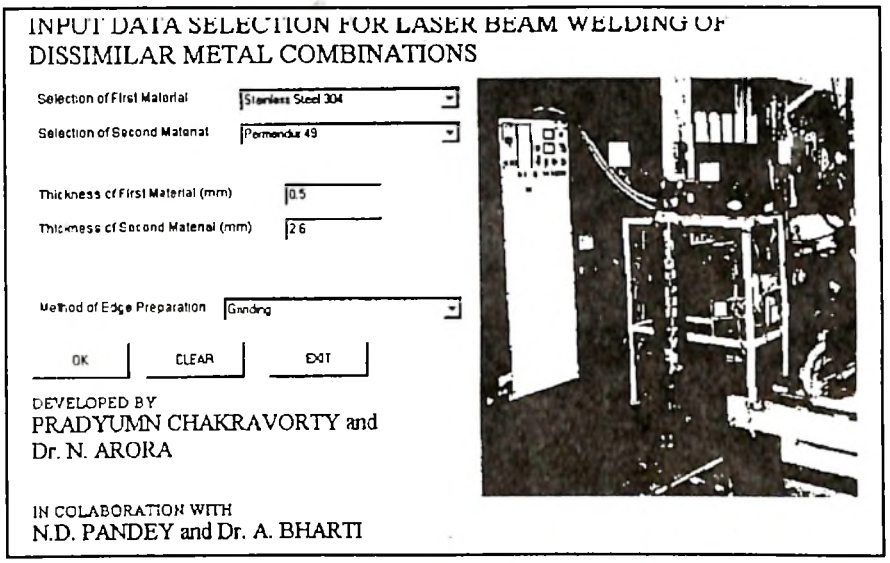

Fig.14 : Data input screen of the expert system

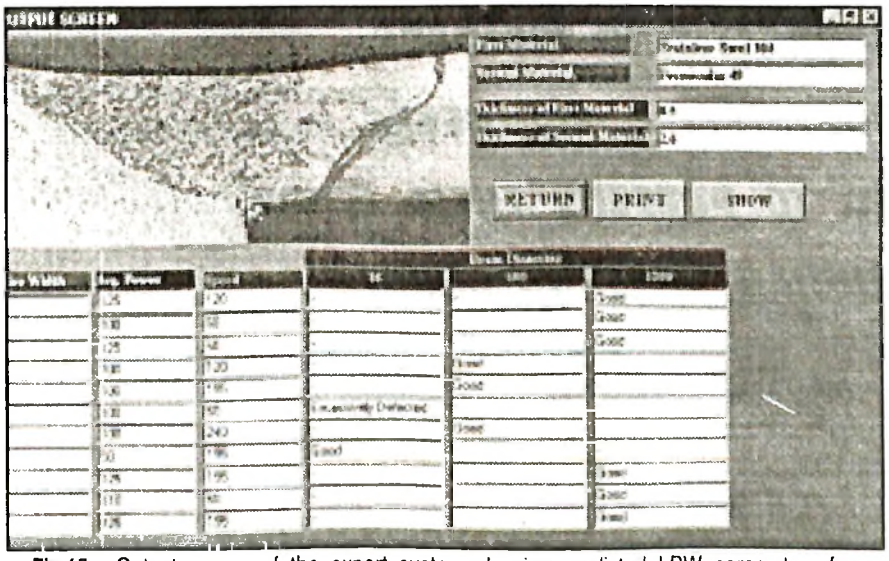

Fig.15 : Output screen of the expert system showing predicted LBW parameters for welding of SS-304 and P-49

7. W.W. Duley, Laser Welding, John Wiley & Sons, Inc., 1999, pp. 1-63.
8. W.M. Steen, Laser Material Processing, Springer-Verlag, London, U.K., 1991, pp. 108-144.
9. Welding Handbook, 7th Ed., Vol. 3, A.W.S., Florida, U.S.A., 1980, pp. 169-214.
10. N.D. Pandey and A. Bharti, in Conf. Proc. International Welding Conference, New Delhi, February 2001, pp. 1127-1143.
11. N.D. Pandey and A. Bharti, DMRL Technical report, TR 98225, 1998.
12. C.Y. Yeo, S.C. Tam, S. Jana, M.W.S. Lau, J. Mat. Proc. Tech., 42,1994, pp.l5-49.
13. J. Mazumder, J. of Metals, 34(7), 1982, pp. 16-24
14. M. von Allmen and A. Blatter, Laser Beam Interaction with Materials, 2nd Ed., Springer-Verlag, New York, U.S.A., 1995.
15. I. Miyamoto, H. Maruo and Y. Arata, in Plasma, Electron and Laser Beam Technology, Ed. Y. Arata, American Society of Metals, OH, U.S.A., 1986, pp. 492-497.
16. A. Matsunawa, H. Yoshida and S. Katayama, in Proc. ICALEO' 84, Ed. J. Majumder, 44, 1984, pp. 35-42.
17. F.P. Gagliano and V.J. Zaleckas, in Laser in Industry, Ed. SS

Charschan, Van Nostrand Reinhold Co., N.Y., U.S.A., 1972, pp. 191-294.

18. W.W. Duley, Laser Processing and Analysis of Materials, Plenum Press, N.Y., U.S.A., 1983, pp. 69-176.

19. R.S. Patel, The Role of an Assist Gas during Laser Metal Interaction, Ph.D. Thesis, Univ. of Illinois at Urbana Champaign, U.S.A., 1989, p.33.

20. P. Chakravorty, N.D. Pandey, N. Arora and A. Bharti, in Proc. 13th Annual General Meeting of MRSI, Hyderabad, February 2002, p. A12.

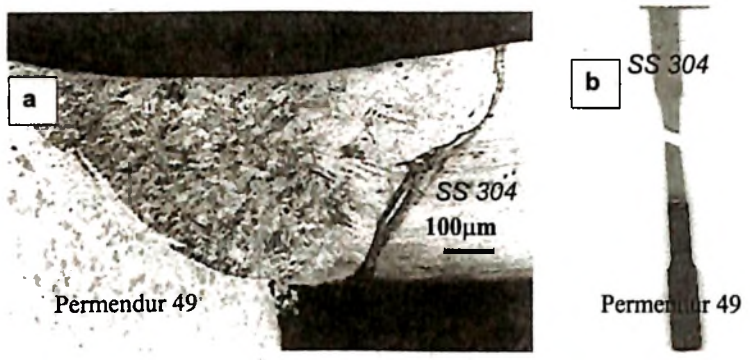

Fig.16 : Dissimilar metal weld produced using predicted LBW parameters of Sl. No. 3 of the output screen of the expert system (a) microstructure and (b) tested tensile specimen.

Attention !!!

YOUNG PRACTISING WELDERS, TECHNOLOGISTS & ENGINEERS ARE INVITED TO PRESENT THEIR WORK IN THE INDIAN WELDING JOURNAL

– EDITOR, IWJ